

Evaluating Air-Water and NAPL-Water Interfacial Adsorption and Retention of Perfluorocarboxylic Acids within the Vadose Zone

Jeff A. K. Silva^{1*}, William A. Martin³, Jared L. Johnson³, John E. McCray²

¹GSI North America, Inc., 17 Chruch Street, Flemington, NJ, 08822, USA; jsilva@gsisg.com

²Civil & Enviromental Engineering Department, Hydrologic Science and Engineering Program,
Colorado School of Mines, 1500 Illinois Street, Golden CO, 80401, USA

³U.S. Army – Engineer Research and Development Center (ERDC), 3909 Halls Ferry Road,
Vicksburg, MS, 39180, USA

Manuscript Submitted to *Journal of Contaminant Hydrology* as a Research Article
(PFAS Special Issue).

Abstract

The release and transport of linear perfluorocarboxylic acids (PFCA) within the vadose-zone beneath per- and polyfluoroalkyl substance (PFAS)- and non-aqueous phase liquid (NAPL)-contaminated source areas is influenced by multi-phase interfacial retention phenomena. Conceptually, interfacial adsorption results in retardation of PFCA velocities in subsurface multiphase systems. However, site hydrochemical factors influencing interfacial adsorption are not yet fully elucidated. Herein, air-water and NAPL-water interfacial tension isotherms were prepared for six homologous PFCAs of environmental significance for deionized water and five synthetic groundwaters of increasing ionic strength. The isotherms were successfully modeled by the Langmuir-Szyskowski equation and parameters used to fit the measured data are provided. Concentration-dependent interfacial adsorption coefficients and retardation factors are also provided for each PFCA and ionic strength condition and are evaluated to assess their significance. Simplifying relationships for predicting interfacial adsorption based on PFCA chain length were found to be less appropriate for natural groundwaters that contain a mixture of dissolved divalent and monovalent ions. Air-water interfacial (AWI) adsorption increased in a threshold manner with ionic strength from 0 to 6 mM, whereafter further adsorption was marginal. PFCA retention within water-unsaturated porous media is shown to depend on a number of inter-related factors and conditions that complicate the use of retardation factors within analytical models typically used for predicting transport rates under field conditions. Numerical simulation is thus necessary to model fundamental fate and transport processes. Mathematical relationships for incorporating interfacial adsorption in future and existing unsaturated flow and transport models are described.

Key Words: PFAS, perfluorocarboxylic acid, surface tension, vadose zone, air-water interfacial adsorption, NAPL-water interfacial adsorption.

1. Introduction

The extensive use of aqueous film forming foams (AFFF) for fuel fire suppression, and releases during equipment testing and training activities since the 1960's, has resulted in widespread contamination of groundwater resources, surface waters, and soils by per- and polyfluoroalkyl substances (PFAS) at both military and civilian facilities (e.g., Moody and Field, 2000; Moody et al., 2003; Filipovic et al, 2015; Anderson et al., 2016). AFFF formulations are a complex mixture of chemicals that can include 1-4% w/w PFAS, and is supplied as a solution concentrate that is typically diluted to a 3-6% v/v for use in fire suppression. When released at ground surface, AFFF solutions can infiltrate into the shallow subsurface, allowing PFAS contamination to initially transport through a vadose zone, where PFAS can be retained before impacting groundwater. In some locations the vadose zone extends just a few feet below ground surface. However, at release locations in the western and southwestern United States (US), the extent of the vadose zone can be significant (e.g. hundreds of feet), providing conditions for longer-term retention of these chemicals in the vadose zone environment.

The potential for PFAS in the vadose zone to serve as a long-term source of groundwater contamination has been recently identified from field-scale evaluations (Shin et al., 2011; Xiao et al., 2015; Weber et al., 2017; Anderson et al. 2019). For example, based on site data, Weber et al (2017) concluded that PFAS contamination within the vadose zone beneath a former military fire training area continues to be a source of groundwater contamination some 18 years after training operations had ceased. PFAS are also components of many industrial waste and consumer products that can leach and transport within both water-saturated and unsaturated portions of

municipal and commercial landfills, which can also serve as a long-term source of groundwater contamination. Therefore, it is important to understand and characterize the mechanisms of transport of PFAS within the vadose zone environment to better assist risk-based assessments and remedial action decision making.

PFAS of interest in our research are the perfluoroalkyl acids (PFAA), and specific to this current work the perfluoroalkyl carboxylates (PFCAs) which are anionic surface-active agents (i.e. surfactants). These chemicals have been identified as both components of some current and legacy AFFF formulations and degradation products of precursory AFFF components (Moody and Field, 2000; Houtz et al., 2013; Weber et al, 2017). PFAA retardation during transport in the vadose zone can occur as a result of a combination of retention mechanisms, including adsorption to soil surfaces as mineral adsorption or association with bound organic phases (Higgins and Luthy, 2006; Guelfo and Higgins, 2013) and adsorption to air-water interfaces (AWIs) within the water-unsaturated porous matrix (Brusseau, 2018; Lyu et al, 2018). Partitioning from the aqueous phase to the soil gas phase is not considered to be of significance for the PFCAs, as these compounds will be dissolved as anions under typical environmental pH conditions when in dilute solution (Goss, 2008; Vierke et al., 2013). For AFFF source zones, PFAS partitioning to co-disposed non-aqueous phase liquids (NAPL) (e.g. hydrocarbon fuels and/or solvents) and adsorption at NAPL interfaces have also been suggested as a potentially significant PFAS retention mechanisms (Guelfo and Higgins, 2013; McKenzie et al., 2016).

While AWI and NAPL-water interfacial (NWI) adsorption has been considered in the recent environmental literature, the significance of these retention mechanisms to the transport of PFAS in real vadose zone environment remains ambiguous. Brusseau (2018) presented a comprehensive retention model for PFAS, that included the retention contributions of solid-

94 phase sorption, AWI/NWI adsorption, partitioning between the aqueous and gas phases, and
95 NAPL-water partitioning. This modeling approach, and its component processes, was developed
96 and evaluated by many researchers during the 1990s and early 2000s to describe hydrocarbon
97 and hydrocarbon-based surfactant fate and transport (e.g., Brusseau et al., 1992; Brusseau et al.,
98 1997; Kim et al., 1997, Silva, 1997, Kim et al., 1998; Costanza and Brusseau, 2000, Kim et al.,
99 2001; Silva et al., 2002) and was recently modified by Brusseau (2018) to describe PFAS
100 retention in porous media.

101 Specific to AWI adsorption, Brusseau (2018) demonstrated that this mechanism alone could
102 account for up to 50% of the total retardation of perfluorooctanoic acid (PFOA) for an assumed
103 constant volumetric moisture content and AWI area condition. Likewise, Lyu et al (2018)
104 performed unsaturated column experiments to demonstrate that AWI adsorption alone accounted
105 for 50 – 75% of the total retardation of PFOA, depending on the aqueous concentration of
106 PFOA, which in this case ranged between 0.01 and 1 mg/L. Using AWI adsorption coefficients
107 (k_{ia}) developed from surface tension isotherm data extracted from a figure originally presented
108 by Lunkenheimer et al. (2015) for the C6-C11 PFCA homologues (sodium salts), Lyu et al
109 (2018) go on to demonstrate that AWI adsorption, as a mechanism for retention, is significant
110 only for PFCAs > C8. However, this result is somewhat misleading as the data used to develop
111 the adsorption coefficients were for PFCA solutions prepared in deionized water. It is well
112 known that solution ionic strength and ionic composition affects, and often enhances, the degree
113 of adsorption of both ionized hydrocarbon and fluorocarbon surfactants at the AWI (Downes, et
114 al., 1995; Kissa, 2001; Gurkov et al., 2005).

115 With respect to NWI adsorption, the significance of this mechanism and its contribution to the
116 overall retention of PFAS in vadose zone and saturated zone is less certain. While it has been

shown that perfluorocarbon surfactants exhibit some affinity for hydrocarbon-water surfaces (Mukerjee and Handa, 1981), little experimental data exists to properly evaluate NWI adsorption for specific NAPLs associated with AFFF training areas (e.g. trichloroethene (TCE) and diesel/aviation fuels). Further, as a part of parameterizing their aforementioned model, Brusseau (2018) addressed NWI adsorption by assuming NWI adsorption coefficients (k_{ni}) and k_{ia} values were equivalent, based on ancillary observations of adsorption coefficient equivalence for hydrocarbon surfactants. Using a constant NWI area (A_{ni}), and the same soil moisture conditions assumed for the AWI calculation, this analysis indicated that NWI partitioning provided a 15% contribution to the total retardation of PFOA in this system. However, the assumption of equivalent NWI and AWI adsorption coefficients is not entirely satisfying given that previous research has demonstrated that NWI adsorption of both hydrocarbon surfactants (i.e. sodium dodecyl sulfate) and PFCA surfactants on non-polar NAPL surfaces are less than that observed for adsorption at the AWI, (Mukerjee and Handa, 1981; Gurkov et al., 2005). Although Brusseau (2018) acknowledge the potential for disparity between k_{ia} and k_{ni} values for perfluorocarbon surfactants based on physicochemical property differences, additional research is needed to rightly quantify NWI adsorption coefficients to support fate and transport calculations at PFAS source areas.

In this present work we address the limitations existing within the current literature dataset relating to fluid-fluid interfacial adsorption and its significance as a mechanism of retention within water-unsaturated porous media. Aqueous surface tension isotherms were prepared for 6 homologous PFCAs and 5 simulated groundwaters of varying ionic strength. NWI tension isotherms were also prepared for TCE and kerosene as NAPL phases, with kerosene serving as a surrogate for aviation-type fuels commonly used at AFFF training sites. Concentration dependent

k_{ia} and k_{ni} values are presented and used to demonstrate the significance of AWI and NWI adsorption as a source of retention and their impact on transport and storage of these contaminants in the vadose zone. A discussion of the applicability of the retardation factor for estimating PFCA transport in water-unsaturated porous media is provided. Finally, a possible framework for implementing interfacial adsorption in unsaturated flow and transport models is presented.

2. Materials and Methods

2.1 Materials

Except for kerosene all chemicals were purchased from Sigma-Aldrich Co. and used without further purification. Perfluoropentanoic acid (PFPeA, 97% purity), perfluorohexanoic acid (PFHxA, 98%), perfluoroheptanoic acid (PFHpA, 99% purity), PFOA (96% purity), perfluorononanoic acid (PFNA, 97% purity), and perfluorodecanoic acid (PFDA, 95% purity), were selected as representative linear PFCAs. The free acid form of these PFCAs were selected to mirror that produced in situ by the degradation and/or oxidation of precursor compounds. Deionized (DI) water used in this work conformed to the American Society for Testing and Materials (ASTM) Type II specification. Sodium bicarbonate (NaHCO_3), calcium sulfate ($\text{CaSO}_4 \cdot 2\text{H}_2\text{O}$), magnesium sulfate (MgSO_4), and potassium chloride (KCl) salts were used to prepare solutions of simulated groundwater (SGW). TCE (ACS Reagent Grade) and kerosene (1-K Grade) were used for NWI measurements.

2.2 Methods

2.2.1 Solutions Preparation

SGW solutions were prepared from DI water in batches representing five different ionic strengths, as shown in Table 1. The range of water quality parameters was selected to mimic a

range of values typical of natural groundwaters (U.S. EPA, 2002). From these solutions, individual PFCA test solution standards were prepared within 100 mL high-density polyethylene bottles. The preparations slowly agitated for 48 hours prior to use. DI water PFCA standards were also similarly prepared.

NWI standards were prepared by adding 15 mL of NAPL and 15 mL of aqueous PFCA solution into 60 mL clear glass jars. TCE-PFCA solution standards were prepared by first adding TCE to the jar followed by PFCA solution to the TCE surface. Conversely, the kerosene-PFCA standards were prepared by adding the aqueous PFCA solutions to the test jars first, followed by kerosene as the less dense phase. The dual-phase preparations were allowed to stabilize for a period of 48 hours prior to use.

Table 1. Characteristics of Synthetic Groundwaters

	Reagent Salt Added (mg/L)				Water Quality Parameters		
	NaHCO ₃	CaSO ₄ ·2H ₂ O	MgSO ₄	KCl	TDS (mg/L)	pH	Ionic Strength (M)
SGW-1	12	7.5	7.5	0.5	27.5	6.8	0.006
SGW-2	48	30	30	2	110	7.3	0.023
SGW-3	96	60	60	4	220	7.8	0.046
SGW-4	192	120	120	8	440	8	0.092
SGW-5	384	240	240	16	880	8.4	0.183

2.2.2 Aqueous Surface Tension Measurements and AWI Adsorption Coefficients

Surface tension measurements were made with a du Nouy ring tensiometer (Fisher Surface Tensiomat, Model 21, Fisher Scientific) using standard ring methods (ASTM, 1989). The tensiometer was calibrated using manufacturer-recommended methods. Measurements were repeated over the course of one hour until the measured tension deviated within 1% across three consecutive measurements. Measurements were made using solution standards prepared to

characterize complete surface tension isotherms, up to and including the monomer solubility limit – as determined from surface tension measurement stabilization. However, given that the observed range of PFCA concentration values observed at PFAS-impacted sites is much less than the solubility limit for these surfactants, the range of tension values for PFCA concentrations between 0 and 100 mg/L are presented. Within this range of concentrations solution pH did not fall below a value of 6 in all cases. The results of these measurements were used to construct isotherms of surface tension (γ) versus bulk aqueous concentration (C_w).

The following form of the Langmuir-Szyszkowski (LS) equation was selected to fit the data as (Adamson and Gast, 1997):

$$\gamma = \gamma_0 - b \ln \left(1 + \frac{C_w}{a} \right) \quad [1]$$

where γ_0 is the surface tension of water at the ionic strength of interest, and a and b are fitting parameters. Equation 1 was fit to the data utilizing the Microsoft Excel solver function (i.e., generalized reduced gradient method) and minimizing the sum of the squared error between measured and predicted values. The data fit was then used in all further analyses as it provided a data set of higher resolution for calculating interfacial parameters.

AWI adsorption coefficients (k_{ia} , units of cm^3/cm^2 or cm) were calculated using the following form of the Gibbs equation (Kim et al., 1997; Szymczyk and Janczuk, 2007):

$$k_{ia} = \frac{\Gamma}{C_w} = -\frac{1}{RT} \left(\frac{\delta \gamma}{\delta C_w} \right)_T \quad [2]$$

where Γ is the surface concentration (mole or mass per unit area), R is the universal gas constant and T is the temperature of measurement. This procedure involved calculating the incremental change in the slope of the fitted tension isotherm data (i.e. $\Delta\gamma/\Delta C_w$) across the range of solution

concentrations of interest and applying Equation 2. Lyu et al. (2018) have previously demonstrated, by comparison with the results of transport experiments, that measured surface tension isotherms can be used to predict AWI adsorption coefficients and estimate retardation factors for AWI adsorption in porous media.

With respect to the data fit, it should be noted that this approach utilizes measured data at higher aqueous concentrations, and the surface tension of water at zero PFCA concentration, to anchor the fit of the LS-equation. Thereafter, the approach relies on model interpolation to ultimately calculate interfacial adsorption parameters at concentrations below the limit of discernment in surface tension measurement (i.e. < 5 mg/L for PFPeA, PFHxA and PFHpA; < 1 mg/L for PFOA; < 0.1 mg/L for PFNA and PFDA). Therefore, it is assumed that the LS-equation continues to appropriately describe surface tension reductions due to AWI adsorption at lower concentrations consistent with those observed at field sites.

2.2.3 NWI Tension Measurements

NWI tension measurements were also performed using standard ring methods (ASTM, 1989) and the same du Nouy ring tensiometer referenced in Section 2.2.2. Briefly the measurement method consisted of positioning the du Nouy ring within the PFCA solution phase and, in the case of kerosene, slowly lifting the ring into the NWI and recording the measured tension required to rupture the interface. Similarly, the TCE-PFCA solution systems recorded the tension required to rupture the interface when a downward force is applied on the interface (i.e. du Nouy ring “pushed” into TCE phase). The LS-equation (Equation 1) was again used to fit the measured data, with γ_0 in the present case being the interfacial tension of the NAPL-water system in the absence of PFCA.

Concentration-dependent k_{ni} values were again determined from the Equation 1 fit to the measured data using Equation 2 and the procedure described in Section 2.2.2.

2.2.4 Evaluating AWI Retention in Porous Media

The retardation factor (R_f) describing the contribution of AWI partitioning under water-unsaturated flow in the vadose zone is as follows (Kim et al, 1998):

$$R_f = 1 + \frac{k_{ia}A_{ia}}{\Theta_w} = 1 + \frac{k_{ia}A_{ia}}{S_w n} \quad [3]$$

where A_{ia} is the area of the AWI within a given volume of water-unsaturated soil (cm^2/cm^3 or cm^{-1}), Θ_w is the volumetric water content (-), S_w is the water saturation, and n is the media porosity (-). Here, $R_f = 1$ indicates PFCA retention due to AWI adsorption is absent or negligible.

For water-unsaturated porous media, previous research has shown A_{ia} to continue to increase with decreasing S_w until achieving a maximum value near the specific surface area of the solid at extremely low S_w (e.g. Kakare and Fort, 1996; Kim et al., 1997; Silva 1997; Brusseau et al., 1997; Kim et al., 1999; Silva et al., 2002; Costanza-Robinson and Brusseau, 2002; Peng and Brusseau, 2005). The following $A_{ia}(S_w)$ relationship was used in this evaluation (Peng and Brusseau, 2005):

$$A_{ia} = s[1 + (\alpha S_w)^a]^{-b} - c \quad [4]$$

where s is the specific solid surface area and α , b , and c are fitting parameters (which in this case $s = 5200 \text{ cm}^{-1}$, $\alpha = 19.78$, $b = 1.1$, $c = 104$, and $a = 1/(2-b)$). Parameters used by Lyu et al. (2018) were also directly used to calculate retardation factors (i.e., $A_{ia} = 73 \text{ cm}^{-1}$ and $S_w = 0.77$ or $\Theta_w = 0.23$) in this work for comparative purposes. A graphical representation of this $A_{ia}(S_w)$

relationship for a model sand is provided as Figure 1a. A similar $A_{ia}(S_w)$ function was implemented within the HYDRUS unsaturated flow and transport model for simulating environmental colloid interactions with the A_{ia} during transient drainage and imbibition cycles (Bradford, et al 2015).

2.2.5 Evaluating NWI Adsorption and Transport Retardation

The R_f describing the contribution of NWI adsorption under water-unsaturated flow in the vadose zone is as follows (Saripalli et al., 1998):

$$R_f = 1 + \frac{k_{ni}A_{ni}}{\Theta_w} = 1 + \frac{k_{ni}A_{ni}}{S_w n} \quad [5]$$

where k_{ni} is the NWI adsorption coefficient (cm) and A_{ni} is the area of the NWI. In this evaluation, NAPL contamination occurs as entrapped NAPL ganglia within the porous media. As the non-wetting fluid in a typical vadose zone environment, only a small fraction of the total NAPL area will be exposed to the convecting aqueous phase than would be the case for the AWI at the same soil moisture condition. Therefore, the dependence of interfacial area on S_w for the NWI will differ from that of the AWI. To facilitate this evaluation, the following $A_{ni}(S_w)$ relationship was derived from the main imbibition curve of the computed microtomography measurements for NAPL at residual saturation for the data presented by Porter et al. (2010) as:

$$A_{ni} = d + eS_w + f\sqrt{S_w} \quad [6]$$

where d , e , and f are fitting parameters (which in this case were $d = 10^{-4}$, $e = -1.5$, and $f = 1.5$). NAPL saturation was at residual, or $< 10\%$ as estimated based on reported properties of the sand. A graphical representation of this dataset and the Equation 6 fit to the data used in subsequent calculations is provided as Figure 1b.

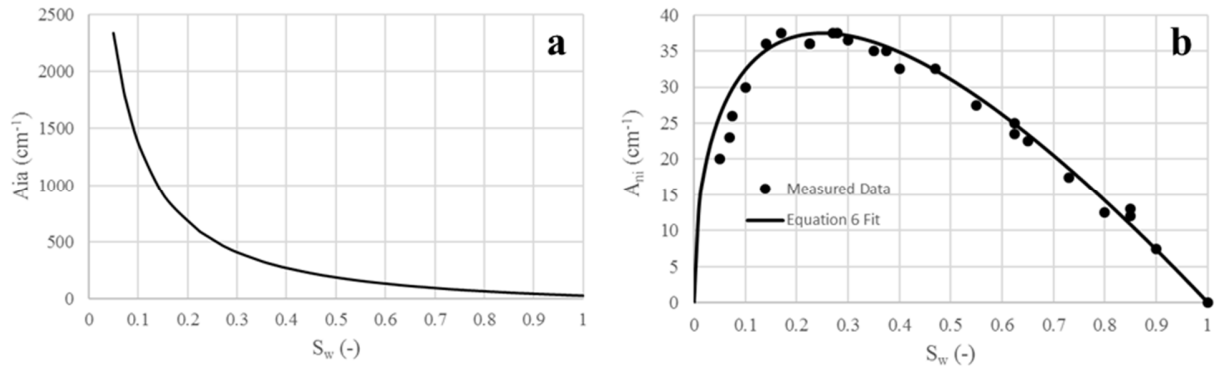


Figure 1. Model water saturation-interfacial area functions used in this work : a) $A_{ia}(S_w)$ and b) $A_{ni}(S_w)$.

3. Results and Discussion

3.1 Surface Tension and AWI Adsorption

Examples of the surface tension isotherms developed in this work are presented in Figure 2 for the DI water solutions and two SGW solutions representing the lowest and highest ionic strengths used in this work. The solid lines in Figure 2 are the modeled tension isotherms resulting from the fit to the measured data. The results of data fitting, including fitting parameters and goodness-of-fit statistics, are presented as in Table 2. Equation 1 was found to well represent the measured surface tension isotherms across the range of PFCA solution concentrations utilized. To our knowledge, k_{ia} values for PFCA contaminants in solutions representing natural groundwater geochemistry have not yet been reported.

Complete PFCA-specific surface tension isotherms can be reproduced using the a and b parameters presented in Table 2, and Equation 1. The high concentration limit is where C_w provides the minimum tension (γ_{min}) and the low concentration limit being $C_w = 0$. k_{ia} values can then be determined at a specific aqueous concentration of interest from the slope of the isotherm at that concentration and Equation 2. These surface tension isotherms have value not only for the purposes of this presentation, but also for environmental calculations involving

estimating PFCA mass associated with aqueous aerosols or potential removal efficiencies for remediation technologies that rely on AWI adsorption to air bubbles to remove PFCA mass from the aqueous phase.

The results presented in Figure 2 exhibit some anticipated trends. Measured aqueous surface tensions were observed to decrease with increasing PFCA solution concentration and with increasing number of $-\text{CF}_2-$ groups comprising the monomer chain (i.e. increasing PFCA chain length or carbon number (C_N)) for these homologous chemicals. The corresponding dependence of k_{ia} on PFCA concentration is also provided in Figure 2. k_{ia} values are shown to decrease with increasing PFCA concentration. This trend may initially seem counter-intuitive when considering Γ increases with increasing concentration. However, as k_{ia} represents the equilibrium condition between the PFCA adsorbed at the AWI and that dissolved within the bulk aqueous phase, at very low concentration small increases in C_w result in larger increases in Γ which, by Equation 2, provides a larger k_{ia} .

AWI adsorption was also observed to increase with increasing SGW ionic strength. This result is generally attributed to a hydrophobic effect that combines a reduction in bulk aqueous solubility of the amphiphile and decreased electrostatic repulsion of the ionic portion of the amphiphile when positioned at the AWI (Gurkov et al., 2005). The effect of dissolved electrolytes on surface tension is well known for surfactants and is readily observed in Figure 2. Additional observations related to solution ionic strength and PFCA interfacial adsorption will be addressed in greater detail in a subsequent section.

A summary of k_{ia} values calculated from the surface tension isotherm data developed in this work is provided as Table 3 for a 1 mg/L PFCA solution concentration. The 1 mg/L

concentration was selected for comparison with previous work and generally represents the upper range of values observed at field sites for PFCAs (e.g. fire training areas at Naval Air Station Fallon, NV and Tyndall Air Force Base, FL – Moody and Field, 1999). While there is currently a limited published data set from which to compare these results, Lyu et al (2018) presented k_{ia} values for PFOA, prepared in 0.01M NaCl solution and DI water (2.0×10^{-3} cm and 9.55×10^{-3} cm per the reported regression equation, respectively), that are very similar to those presented in Table 3, where SGW-1 ionic strength was 0.006 M. The regression equation presented by Lyu et al (2018) (i.e. $\log k_{ia} = 0.56C_N - 7.5$) described the dependence of k_{ia} on C_N for a homologous series of PFCA sodium salts (solutions prepared in DI water) that were derived from data originally presented by Lunkenheimer et al. (2015). The results of this regression equation are presented in Figure 3a, along with the $k_{ia}(C_N)$ relationships developed for the current dataset.

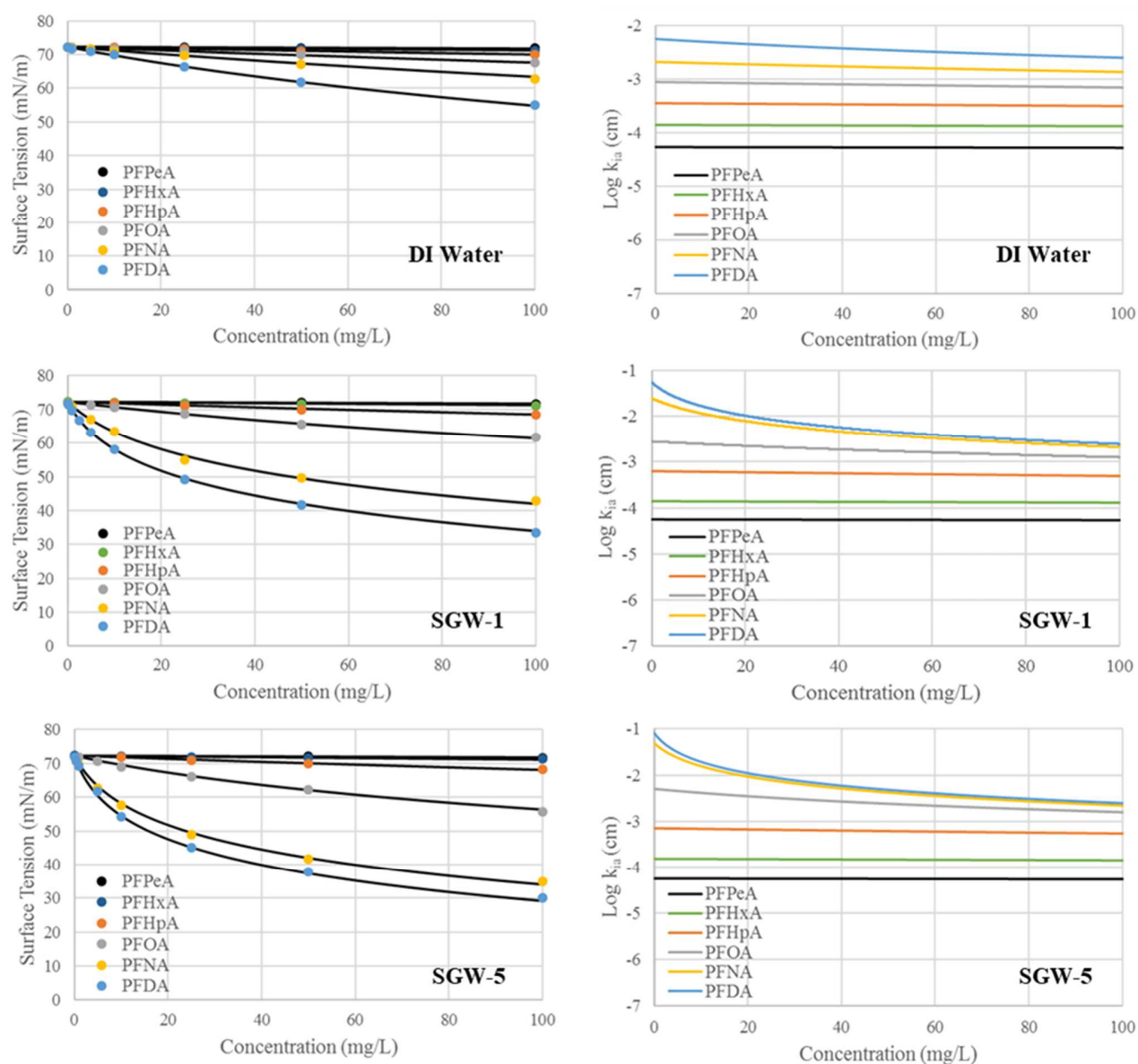


Figure 2. PFCA surface tension isotherms and $\text{Log } k_{ia} C_w$ functions. Black lines in surface tension plots are the LS-Equation fits to the measured data.

Table 2. The results of fitting the LS-Equation to the measured PFCA AWI tension isotherms.

Water	PFCA	Equation 1 Parameters			Goodness of Fit Parameters			
		a	b	γ_{\min} (mN/m)	n	R^2	χ^2	P
DI	PFPeA	1.29E-02	0.22	18.7	11	0.997	0.022	1
	PFHxA	5.40E-03	0.26	17.2	10	0.999	0.002	1
	PFHpA	2.10E-03	0.27	18.4	10	0.998	0.011	1
	PFOA	8.97E-04	0.27	16.5	9	0.999	0.031	1
	PFNA	4.00E-04	0.29	21.2	8	0.998	0.011	1
	PFDA	1.57E-04	0.30	22.9	9	0.998	0.007	1
SGW-1	PFPeA	1.20E-02	0.22	18.7	9	0.997	0.026	1
	PFHxA	4.40E-03	0.21	17.2	10	0.998	0.014	1
	PFHpA	1.00E-03	0.22	18.4	7	0.997	0.019	1
	PFOA	2.00E-04	0.19	14	7	0.998	0.022	1
	PFNA	1.50E-05	0.16	13.9	7	0.998	0.034	1
	PFDA	9.50E-06	0.17	26.2	6	0.996	0.019	1
SGW-2	PFPeA	1.20E-02	0.22	18.7	10	0.997	0.041	1
	PFHxA	4.30E-03	0.21	17.2	10	0.998	0.021	1
	PFHpA	9.50E-04	0.22	18.4	8	0.999	0.012	1
	PFOA	1.50E-04	0.19	13.9	7	0.998	0.023	1
	PFNA	1.10E-05	0.16	13.9	7	0.997	0.014	1
	PFDA	7.20E-06	0.17	25.7	6	0.996	0.039	1
SGW-3	PFPeA	1.20E-02	0.22	18.7	11	0.999	0.002	1
	PFHxA	4.20E-03	0.21	17.2	10	0.999	0.001	1
	PFHpA	9.20E-04	0.22	18	7	0.999	0.027	1
	PFOA	1.30E-04	0.19	13.5	7	0.997	0.037	1
	PFNA	9.50E-06	0.16	13.9	7	0.999	0.003	1
	PFDA	6.00E-06	0.17	24.2	7	0.998	0.012	1
SGW-4	PFPeA	1.20E-02	0.22	18.7	9	0.998	0.012	1
	PFHxA	4.00E-03	0.21	17.2	11	0.997	0.042	1
	PFHpA	9.10E-04	0.22	18	6	0.999	0.055	1
	PFOA	1.20E-04	0.19	13	7	0.999	0.016	1
	PFNA	8.90E-06	0.16	13.9	7	0.999	0.004	1
	PFDA	5.00E-06	0.17	22.2	7	0.998	0.021	1
SGW-5	PFPeA	1.20E-02	0.22	18.7	9	0.998	0.015	1
	PFHxA	4.00E-03	0.21	17.2	10	0.998	0.11	1
	PFHpA	9.08E-04	0.22	18	7	0.999	0.009	1
	PFOA	1.10E-04	0.19	13	7	0.999	0.011	1
	PFNA	8.50E-06	0.16	19.8	7	0.999	0.040	1
	PFDA	4.70E-06	0.17	22.2	9	0.999	0.085	1

Note: a (mol/L) and b (°) are the fitting parameters for the Szyszkowski Equation fit to the measured data, k_L is the Langmuir coefficient, γ_{\min} is the minimum surface tension for these measurements, n is the number of measurements, R^2 is the regression coefficient, χ^2 is the chi-square statistic, and P is the probability statistic.

Table 3. Example AWI adsorption coefficients for 1 mg/L PFCA solutions.

Water	PFPeA (C5)	PFHxA (C6)	PFHpA (C7)	PFOA (C8)	PFNA (C9)	PFDA (C10)
DI	4.97E-05	1.30E-04	3.75E-04	8.83E-04	2.07E-03	5.51E-03
SGW-1	5.35E-05	1.39E-04	6.25E-04	2.74E-03	2.55E-02	4.53E-02
SGW-2	5.35E-05	1.42E-04	6.67E-04	3.68E-03	3.55E-02	5.93E-02
SGW-3	5.35E-05	1.46E-04	6.95E-04	4.30E-03	4.00E-02	6.73E-02
SGW-4	5.35E-05	1.53E-04	7.03E-04	4.60E-03	4.22E-02	6.73E-02
SGW-5	5.35E-05	1.53E-04	7.05E-04	4.93E-03	4.11E-02	6.66E-02

Note: k_{ia} values have units of cm^3/cm^2 or cm .

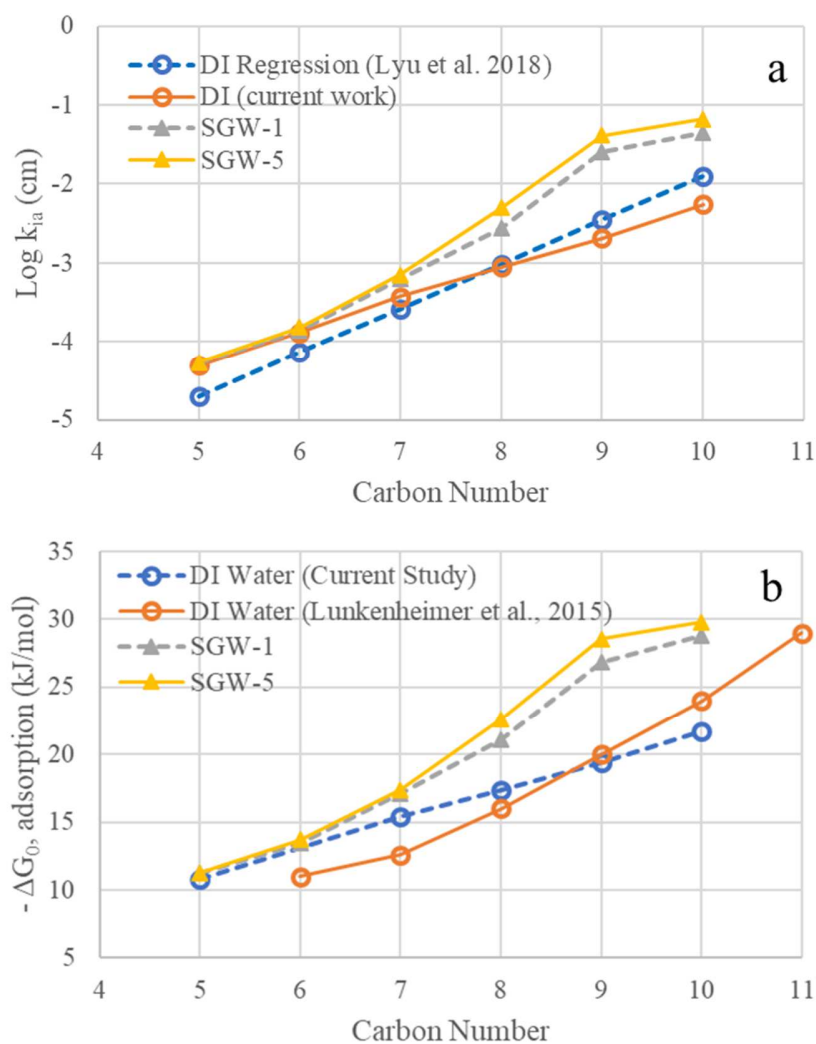


Figure 3. PFCA AWI adsorption coefficients for the 1 mg/L solutions (a) and standard free energy of adsorption (b) as a function of amphiphile chain length or carbon number.

333
334 For the DI water cases, calculated k_{ia} values present log-linearly with increasing C_N . As
335 shown, the slope of the $\log k_{ia}(C_N)$ relationship for the DI water solutions prepared in the
336 current work deviates from that prepared by Lyu et al (2018). We attribute this difference to
337 counterion effects and the use of PFCA sodium salts by Lunkenheimer et al. (2015). In contrast,
338 $\log k_{ia}(C_N)$ for the SGW solutions exhibit a positive deviation from a log-linear trend that
339 increases slightly with increasing C_N between $C_N = 5$ and 9. Beyond $C_N = 9$, the $\log k_{ia}(C_N)$
340 appears to plateau. Repeated solutions preparation and subsequent surface tension measurements
341 indicate the reduced AWI adsorption for PFDA is real for all SGW solutions. It is possible that
342 impurities in the PFCA reagents selected could have contributed to these results. However, given
343 the linearity observed in the $\log k_{ia}(C_N)$ relationship for the DI water cases, the observed
344 deviation from log-linearity observed for the SGW solutions is more likely related to the
345 presence of dissolved ions in solution and concomitant electrostatic effects at the AWI.

346 While the exact mechanism responsible for this observed behavior is not entirely clear, some
347 explanation can be gleaned from a few relevant literature sources. For example, Lunkenheimer et
348 al. (2015), using highly purified sodium-PFCA homologues, observed a non-linear increasing
349 trend in the free energy of AWI adsorption (ΔG_0^{ads}) with increasing C_N that may help to explain
350 some of the non-linearity in the SGW $\log k_{ia}(C_N)$ function. These authors argued that the non-
351 linearity in the $\Delta G_0^{ads}(C_N)$ relationship was due to variability in the Debye screening length of
352 the electrostatic double layer established at the AWI that allows an incrementally increasing
353 adsorption with increasing PFCA C_N that is in excess of that due to amphiphilic nature of these
354 molecules alone. As shown in Figure 3b, this incrementally increasing adsorption phenomenon

may be occurring for the SGW cases. For comparison with the present work, ΔG_0^{ads} was calculated as (Lunkenheimer et al, 2015):

$$\Delta G_0^{ads} = -RT \ln a_L \quad [7]$$

where a_L is the surface activity determined as fitting parameter a in the Equation 1 fits to the surface tension isotherms. In the absence of a counterion electrolyte, the $\Delta G_0^{ads}(C_N)$ relationship for the free acid PFCAs presents as a linear function across the range of C_N investigated. However, in the presence of available counterions, a similar degree of upward curvature is observed in both datasets. In Figure 3b, ΔG_0^{ads} is enhanced for the SGW solutions in response to the elevated ionic strength of the SGW solutions.

Additionally, the Lunkenheimer et al. (2015) dataset presented in Figure 3b combines the results for both even and odd numbered PFCA amphiphile carbon numbers, which were presented separately in their original manuscript. These authors further demonstrated variability in the magnitude of PFCA AWI adsorption that is dependent on whether the PFCA contains an even or odd number of carbons in the chain. Psillakis et al (2009) also observed differing degrees of AWI adsorption for both the PFCAs and perfluoro-n-alkyl sulfonates when C_N was odd or even. These results suggest that an additional cause of the non-linearity observed in the SGW log $k_{ia}(C_N)$ dataset may be related to inherent differences in surface activity between odd and even homologues that manifest more intensely when an excess of dissolved ions are present in solution. Irrespective of the actual mechanism(s) at work here, the current results provide additional evidence that log-linear $k_{ia}(C_N)$ relationships may not be appropriate to predict AWI adsorption in natural groundwaters that contain a mixture of divalent and monovalent ions in solution.

3.1.1 Effect of SGW Ionic Strength on AWI Adsorption

The SGW solutions used in this work were selected to include the major ionic species found in natural waters and to cover a reasonably representative range of groundwater ionic strength. Within the limits of measurement, AWI adsorption was observed to increase with increasing ionic strength and is consistent with the hydrophobic effect described previously. However, the effects of amphiphile hydrophobicity appears to have a limit for the SGW solutions used in this work, in that the rate of change of adsorption decreased markedly once a threshold ionic strength condition was achieved. This threshold condition is best observed in Figure 4, where the calculated k_{ia} values are plotted against the ionic strength of the bulk aqueous solution.

For PFPeA and PFHxA, k_{ia} values were found to be less sensitive to changes in ionic strength, within the range of values investigated. However, for PFCAs of higher C_N a clear threshold ionic strength condition exists above which the rate of further increases in k_{ia} is marginal. Gurkov et al (2005) observed a similar threshold stabilization of aqueous surface adsorption of sodium dodecyl sulfate (SDS) in NaCl solutions when the concentration of NaCl exceeded 0.01M. This result is significant in that it potentially simplifies modeling of the effect of ionic strength (I) on k_{ia} . For example, given the results presented in Figure 4, $k_{ia}(I)$ could be modeled directly using a Langmuir-like expression. However, as will be discussed in Section 3.3, an alternative approach that utilizes relationships developed between the LS-Equation parameters is of more practical value. Further, Gurkov et al (2005) described an additional simplification that suggests normalization of the effect of I on interfacial adsorption parameters can be achieved by re-evaluating the surface tension isotherms in terms of the mean ionic activity the solutions. We are currently evaluating this approach for the SGW results presented herein.

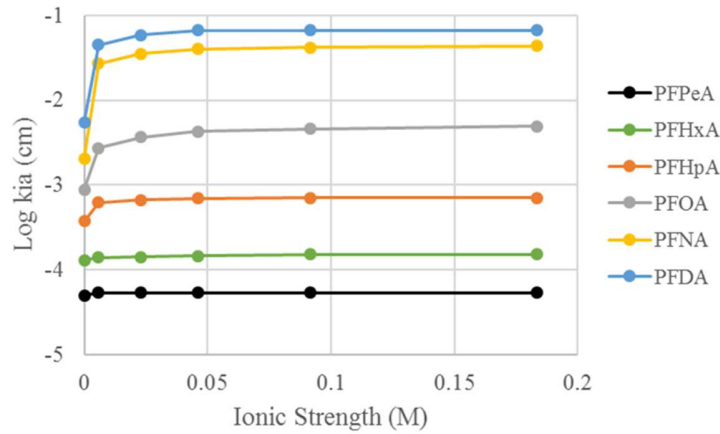


Figure 4. Calculated AWI adsorption coefficients for 1 mg/L PFCA solutions with increasing ionic strength.

3.1.2 Potential Significance of AWI Retention for PFCAs within Vadose Zone Soils

AWI adsorption-specific retardation factors calculated using Equation 3 and the k_{ia} values in Table 2 are presented in Figure 5a for DI water and SGW-1 and SGW-5 solutions as a function of C_N . The analysis utilized the same soil moisture condition and corresponding A_{ia} used by Lyu et al. (2018). The $R_f(C_N)$ relationship developed from the regression equation presented by Lyu et al. (2018) is also provided for comparison.

For these PFCAs, and for all datasets presented in Figure 5a, AWI retention is observed to be minimal for $C_N < 6$. AWI retardation is considerably increased for the SGWs, relative to the DI water cases, due to the increased interfacial adsorption observed for these SGWs. This result is significant and highlights the importance of accounting for groundwater ionic strength when attempting to predict AWI retention. For the SGW cases, R_f values for the higher carbon number homologues are shown to range between 5 and 20. As was observed for the $\log k_{ia}(C_N)$ relationship, the predicted SGW $R_f(C_N)$ relationship deviates from its smoothly increasing function at $C_N = 9$ in response to the stabilization of surface tension observed for the PFDA

isotherms for all SGWs. Similar surface tension stabilization effects were observed for measurements utilizing perfluorododecanoic acid ($C_N=12$, data not shown).

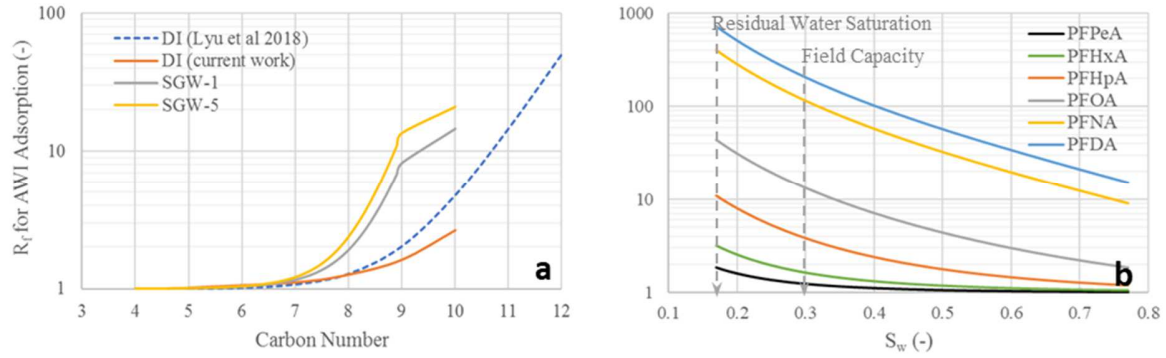


Figure 5. PFCA retardation factors for AWI adsorption as the sole source of retention: (a) R_f values are for $[PFCA] = 1 \text{ mg/L}$ ($A_{ia}=73 \text{ cm}^{-1}$, $S_w = 0.77$ per Lyu et al. (2018)), (b) R_f values possible across a range of soil moisture conditions and for $[PFCA] = 1 \text{ mg/L}$ and SGW-1.

R_f values presented in Figure 5a, were calculated for a single soil moisture condition and a PFCA concentration of 1 mg/L. Additionally, the moisture content condition in this analysis is quite high (i.e. $\theta_w = 0.23$ or 77% of the total pore volume, assuming a porosity of 0.3 for a well sorted sand). Therefore, the results presented in Figure 5a provides a limited assessment of the degree of AWI retention possible. To provide a more comprehensive evaluation, k_{ia} values determined for SGW-1 (Table 2) were used to estimate AWI adsorption-specific R_f values for soil moisture conditions ranging from $S_w = 0.77$ to 0.17 (the assigned residual moisture condition for this hypothetical sand). The results presented in Figure 5b demonstrate the range of R_f values possible for these PFCAs as A_{ia} changes with changes in S_w for a 1 mg/L PFCA solution concentration. For example, at $S_w = 0.77$, a condition potentially met when and while water infiltrates into a volume of vadose zone, the R_f for PFOA is 1.9, whereas R_f increases by at most a factor of 24 at the residual moisture condition. R_f values estimated for the higher

carbon number PFCA homologues at residual moisture were determined to range between 407 and 723.

Given the results presented in Figure 5b, it is clear that these PFCAs should experience a wide range of R_f values within the vadose zone during a given infiltration event, where imbibition and subsequent drainage processes would cause the A_{ia} to vary considerably during the event. Furthermore, during an infiltration event it is likely that the concentration of surfactant in the mobile phase (i.e., convecting aqueous phase) will vary, resulting in variability in k_{ia} values temporally and spatially. The interplay between these variables complicates the typical use of R_f values via Equation 3 (e.g. to directly predict the time of arrival of contaminant at a particular depth in soil) for water-unsaturated flow. Generally, the application of a R_f to characterize the transport of a surface-active chemical under water-unsaturated flow at field-scale is an ill-considered chromatography problem, in which (1) the area of the reactive stationary phase in question (i.e. the AWI) is not constant spatially or temporally under typical field conditions, (2) phase transfer is concentration-dependent and non-linear, and (3) flow of mobile phase is not constant, but rather dynamic and intermittent. This may explain why methods successfully utilizing surface-active tracers to characterize A_{ia} under water-unsaturated flow conditions are typically performed at high and constant water saturation where variability in A_{ia} is minimized and uniform flow can be maintained within the porous medium, and where the surface-active tracer is introduced at a step-input to maintain constant tracer concentration. Numerical methods are likely better suited to resolve the complexity of variables that govern the transport of surface-active contaminants under water-unsaturated flow conditions.

3.2 Potential Significance of NWI Adsorption and Retention

NAPL-water interfacial isotherms for each PFCA prepared for TCE and kerosene as NAPL phases are presented in Figure 6. Again, complete NWI adsorption isotherms were prepared and Equation 1 was used to fit the data. NWI isotherms were prepared for a single SGW composition (i.e. SGW-2), as a similar relative surface/interfacial tension response to ionic strength was expected for both the AWI and NWI. The results of Equation 1 fits to the measured data are provided in Table 4. Equation 1 was again found to well represent the measured NWI tension isotherms across the entire range of PFCA solution concentrations employed. k_{ni} values for a 1 mg/L PFCA solution are presented in Table 6.

As shown in Figure 7, PFCA k_{ni} values were observed to be roughly an order of magnitude lower than those determined for the AWI for all PFCA homologues used in this work. These results are consistent with those previously reported by Mukerjee and Handa (1981) who similarly observed lower adsorption for sodium perfluorooctanoate, from dilute aqueous solution, at the hexane-water interface than was observed at the AWI. This result is not altogether surprising when considering the perfluorocarbon tails of these anionic surfactants are at the same time hydrophobic and oleophobic (Kovalchuk et al., 2014). At the AWI, theory holds that the perfluorocarbon tails of the amphiphile are to be oriented into the air-phase to minimize the overall free energy of the system. On the other hand, the orientation of perfluorinated amphiphiles positioned at the NWI is not as clear. Solvency theory would suggest that the oleophobicity of the perfluorocarbon tails would limit, if not negate, their orientation into the hydrocarbon phase, resulting in lower overall adsorption at the NWI. This theory appears to be supported by the fact that while PFCA k_{ni} values here were found to be the essentially the same for both TCE and kerosene, which possess similar polarity and intermolecular hydrogen bonding

potentials (Hansen, 2007; Batista et al., 2015). k_{ni} values calculated from the data of Mukerjee and Handa (1981) were about a factor of 4 larger for sodium PFOA and PFDA at the hexane-water interface (i.e., 1.5×10^{-2} cm and 2.4×10^{-1} cm, respectively). n-Hexane is a non-polar solvent, with its solvency dependent solely on intermolecular dispersion forces. Therefore, there appears to be a relationship between the degree of NWI adsorption and the solvation properties of the NAPL that warrants additional research. Note also that the $\text{Log } k_{ni}(C_N)$ function exhibits greater linearity compared to the AWI function. This suggests that potential electrostatic screening effects observed for PFCA adsorption at the AWI were not as impactful for NWI adsorption.

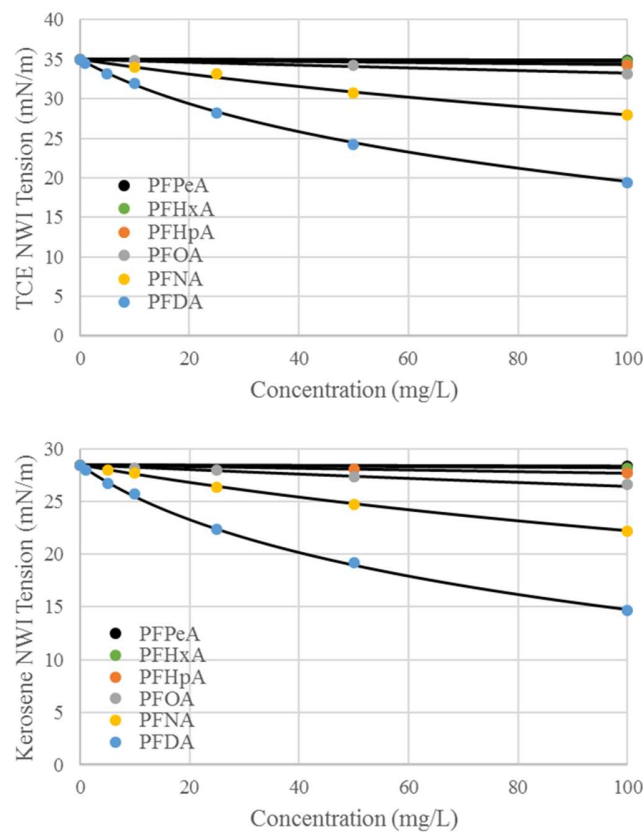


Figure 6. PFCA NWI tension isotherms for TCE and kerosene as NAPL phases. Black lines are the LS-Equation fit to the measured data.

Table 4. The results of fitting the LS-Equation to the measured PFCA NWI tension isotherms (SGW-2).

NAPL	PFCA	Equation 1 Parameters			Goodness of Fit Parameters			
		a	b	γ_{\min} (mN/m)	n	R^2	χ^2	P
TCE	PFPeA	5.50E-02	0.30	15.4	8	0.997	0.05	1
	PFHxA	1.40E-02	0.29	10	8	0.999	0.03	1
	PFHpA	4.00E-03	0.29	13	7	0.998	0.01	1
	PFOA	1.27E-03	0.29	11.2	8	0.996	0.08	1
	PFNA	1.83E-04	0.28	10.4	8	0.998	0.09	1
	PFDA	4.94E-05	0.28	10.4	9	0.996	0.05	1
Kerosene	PFPeA	2.98E-02	0.32	6.8	9	0.998	0.064	1
	PFHxA	9.80E-03	0.31	7.7	7	0.999	0.019	1
	PFHpA	2.89E-03	0.31	8.1	7	0.998	0.051	1
	PFOA	9.02E-04	0.30	9.5	9	0.998	0.033	1
	PFNA	2.00E-04	0.30	8.6	8	0.999	0.025	1
	PFDA	4.23E-05	0.28	6.8	9	0.999	0.046	1

Note: a and b are the fitting parameters for the Szyszkowski Equation fit to the measured data, k_L is the Langmuir coefficient, γ_{\min} is the minimum surface tension, n is the number of measurements, R^2 is the regression coefficient, χ^2 is the chi-square statistic, and P is the probability statistic.

Table 5. NWI adsorption coefficients for 1 mg/L PFCA solutions (SGW-2).

NAPL	PFPeA (C5)	PFHxA (C6)	PFHpA (C7)	PFOA (C8)	PFNA (C9)	PFDA (C10)
TCE	7.60E-06	2.91E-05	1.01E-04	3.16E-04	2.12E-03	7.60E-03
Kerosene	1.25E-05	3.64E-05	1.23E-04	3.86E-04	1.71E-03	7.27E-03

Note: k_{ni} values have units of cm^3/cm^2 or cm .

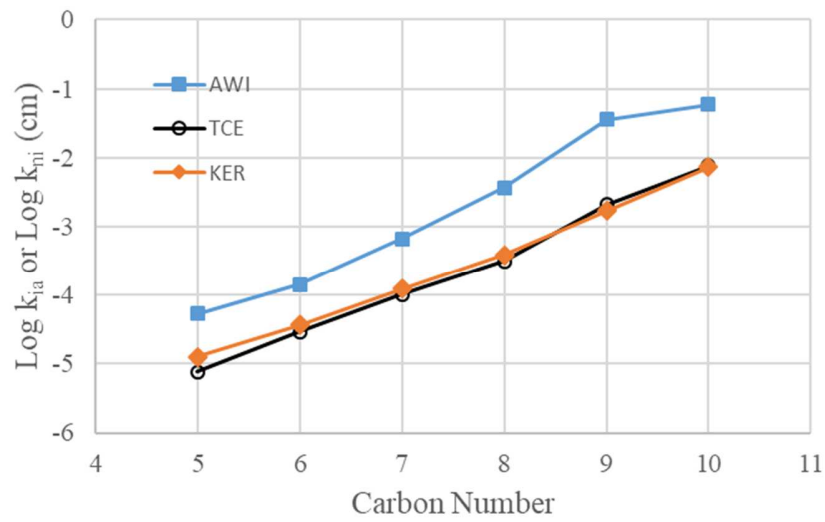


Figure 7. Comparison of $\text{Log } k_{ia}(C_N)$ and $\text{Log } k_{ni}(C_N)$ relationships for AWI and NWI adsorption for 1 mg/L PFCA solutions in SGW-2.

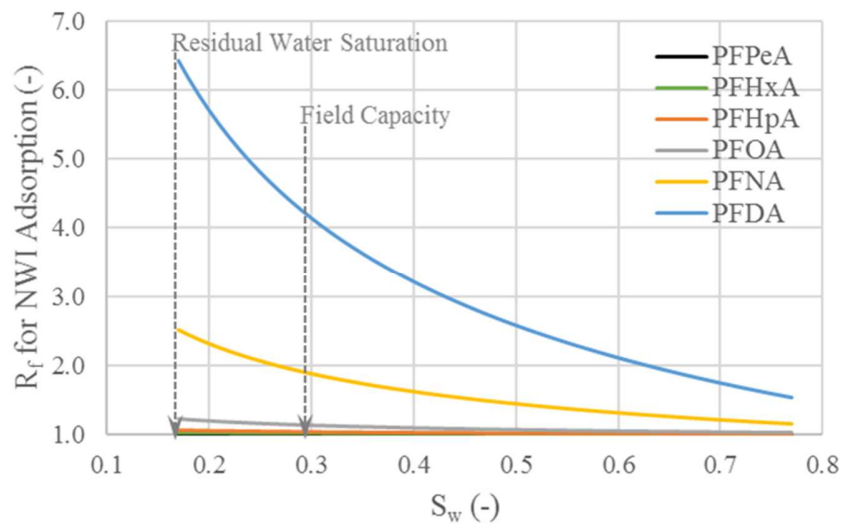


Figure 8. Calculated R_f values for NWI adsorption.

R_f values representing NWI adsorption as a sole source of retention were calculated using Equation 5 and the $A_{ni}(S_w)$ relationship described in Section 2.2.4. Again, the moisture condition limits for this analysis were $S_w = 0.77$ to 0.17 (the assigned residual moisture condition for this hypothetical sand). The results of this analysis are presented in Figure 8, which provides a means of comparing AWI and NWI retention under the same water-unsaturated system conditions.

The combination of the lower k_{ni} values and the lower A_{ni} exposed to the convecting aqueous phase during water-unsaturated flow results in considerably lower R_f values for PFCA transport overall. Calculated R_f values were only appreciably greater than 1 for $C_N > 7$. The NAPL saturation used to develop the $A_{ni}(S_w)$ relationship used in this analysis (Figure 1b) can be considered moderate for this system. For entrapped NAPL ganglia, an increase or decrease in NAPL saturation would be expected to affect R_f values somewhat, but not significantly in that the $A_{ni}(S_w)$ relationship would not be expected to change significantly. R_f decreases with increasing S_w in response to the corresponding decrease in A_{ni} across the range of S_w considered.

It is worth noting that the k_{ni} values and R_f evaluation presented are representative of clean solvents. NAPL contamination beneath PFAS-impacted fire-training areas, for example, would more likely consist of a mixture of co-solvated NAPLs (e.g. waste TCE containing dissolved aviation grease and TCE dissolved in aviation fuel in varied proportion). Therefore, the results of NWI retention calculations presented here should be considered illustrative. However, the observed similarity in PFCA k_{ni} values for both TCE and kerosene (Figure 7) does suggest that

mixtures of these NAPLs would not result in significant differences in individual PFCA k_{ni} values.

3.3. Recommendations for Numerical Simulation of AWI Adsorption

As discussed above, PFCA retention within water-unsaturated porous media depends on factors and conditions that may preclude the use of retardation factors in analytical models typically used for predicting transport rates. Thus, numerical simulation may be necessary to accurately simulate transport for realistic field conditions. Implementing the relevant processes within a numerical model requires tracking interfacial adsorption, $\Gamma(C_w)$, spatially and temporally within a simulation domain, as it relates to A_{ia} , which in turn is determined by the P_c - S_w relationship. The simulator must allow for initializing an ionic strength condition and account for changes in Γ as ionic strength varies within the simulation domain. The simulator would also need to appropriately distribute contaminant mass between the convecting aqueous phase and the AWI in response to changes in aqueous phase concentration, in addition to accounting for other relevant retention processes (e.g. sorption to soils). Finally, AWI adsorption would need to be included in the results of any mass budgeting subroutine.

Here we describe one possible approach to implement AWI adsorption of PFCAs, and potentially other PFAS-related perfluoro-surfactants, within future or existing unsaturated flow and transport simulators. This approach highlights and includes some simplifying relationships observed from the results of this work. Although, facilitating numerical simulation of AWI adsorption is the focus of this discussion, exclusion of other relevant and significant transport mechanisms is not implied. For example, existing unsaturated flow and transport models (e.g. HYDRUS) already account for sorption processes under a variety of potential modes (e.g. as linear, non-linear, one-site/two site kinetic modes) and additional PFAS-specific sorption models

can be easily implemented. However, commercial versions of these existing numerical simulators do not include interfacial adsorption as a retention mechanism. Therefore, the following describes methods to include AWI adsorption as an additionally contributing retention mechanism. NWI adsorption could be similarly implemented if the simulator includes NAPL as a non-wetting reactive phase.

3.3.1 Concentration-Dependent PFCA Adsorption

Because the LS-equation was observed to fit the measured surface tension data, $\Gamma(C_w)$ can be described by the Langmuir adsorption isotherm as:

$$\Gamma(C_w) = \frac{\Gamma_{max} K_L C_w}{1 + K_L C_w} \quad [8]$$

where Γ_{max} is the maximum surface concentration (i.e. at the amphiphile solubility limit) and K_L is the Langmuir coefficient (m^3/mol). The LS-equation, presented as Equation 1, can also be written as:

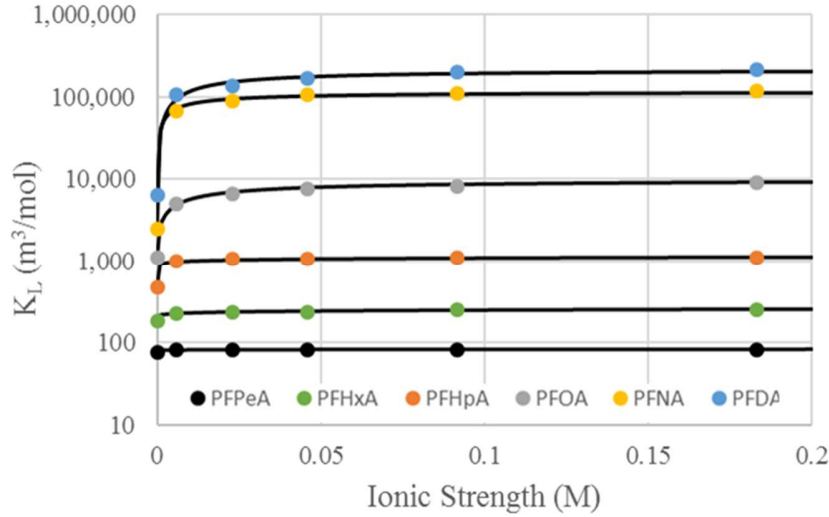
$$\gamma = \gamma_0 - RT\Gamma_{max} \ln(1 + K_L C_w) \quad [9]$$

where parameter b , in Equation 1, is $RT\Gamma_{max}$ and $a = 1/K_L$. As a result, the LS equation parameters provided in Table 2 can be used to parameterize Equation 8 directly.

3.3.2 Ionic Strength Dependence

To model dependence of Γ on ionic strength, relationships observed between the LS equation parameters can also be exploited to help simplify simulation. For example, as shown in Table 2, the fit to the surface tension data resulted in a LS-Equation b -parameter that remained essentially constant for an individual PFCA across the range of ionic strength utilized in this work, a condition that was also observed by Gurkov et al. (2005). Therefore, Γ_{max} for individual PFCAs

570 can be assumed to remain constant. On the other hand, as shown in Figure 9, K_L (as $1/a$) exhibits
 571 a clear trend with increasing I that is similar to those shown for k_{ia} in Figure 4.



572
 573 **Figure 9. $K_L(I)$ relationships for individual PFCAs.**

574 $K_L(I)$ relationships can also be modeled using the following Langmuir-like expression:

$$575 \quad K_L(I) = K_{L,0} + \frac{K_{L,max} b I^n}{1 + b I^n} \quad [10]$$

576 where $K_{L,0}$ is the PFCA Langmuir coefficient for $I=0$ (DI water in this case), $K_{L,max}$ is the
 577 maximum value for the dataset, and b and n are fitting parameters. By implementing Equation
 578 10 directly into Equation 8, the transport simulator would not necessarily need to include a
 579 geochemical simulator to account for changes in AWI adsorption due to variabilities in pore-
 580 water ionic strength.

581 3.3.3 Implementing $P_c - S_w - A_{ia}$ Dependence

582 Existing unsaturated flow simulators generally require parameterization of the relationship
 583 between capillary pressure and water saturation function [$P_c(S_w)$] for the porous medium (e.g.
 584 via van Genuchten and/or Brooks-Corey models). However, to model AWI retention, the P_c - S_w -

A_{ia} relationship is required. Fortunately, these simulators typically calculate P_c and/or S_w at each mesh/grid node and for each numerical time step. Therefore, simple modifications to the code would be required to additionally calculate A_{ia} , spatially and temporally, utilizing existing $A_{ia}(S_w)$ relationships like that presented previously as Equation 4. Equation 4 requires many fitting parameters that are typically specific for a given porous media. However, [Costanza-Robinson et al. \(2008\)](#) developed an empirical $A_{ia}(S_w)$ relationship that greatly simplifies A_{ia} calculation as:

$$A_{ia}(cm^{-1}) = SA[-0.9112S_w + 0.9031] \quad [11]$$

where, SA is the geometric surface area of the media (i.e. sandy soils and sand) calculated as $6(1 - n)/d_{50}$. Equation 11 is based on a smooth-spheres assumption and is therefore most appropriate for sands and sandy soils. However, ongoing research in this area will likely result in similar relationships for additional soil types.

4. Summary and Conclusions

Air-water and NAPL-water interfacial tension isotherms were prepared to determine concentration-dependent adsorption coefficients for 6 homologous linear perfluorocarboxylic acids (PFCA) of environmental interest and for 5 synthetic groundwaters of varying ionic strength. TCE and kerosene (as a surrogate for jet fuel) were used as representative NAPLs, as both are commonly found as co-contaminants at former military fire training areas where AFFFs. The Langmuir-Szyszkowski equation was used to fit the interfacial tension data, and parameters needed to recreate these isotherms for all PFCAs and ionic strength conditions for both air-water and NAPL-water systems are reported in this work. The interfacial adsorption coefficients were

subsequently used to demonstrate the significance of PFCA retention within water-unsaturated soils.

AWI adsorption was observed to decrease as a function of aqueous concentration, a trend consistent with the slope of the AWI tension isotherms. AWI adsorption was also observed to increase with increasing ionic strength and with increasing PFCA carbon number. While log-linear relationships between adsorption and amphiphile carbon number are convenient for predictive purposes, we found that these relationships did not hold for the synthetic groundwaters used in this research and conclude that they could be less reliable for natural groundwaters, where a mixture of divalent and monovalent ions typically exist in solution. However, a log-linear relationship based on PFCA carbon number were observed for the NAPL-synthetic groundwater systems.

Retardation factors for both AWI and NWI adsorption of individual PFCAs increased exponentially with increasing PFCA carbon number. Retardation factors for NWI adsorption were altogether lower than those for the AWI, as a result of lower interfacial adsorption coefficients and lower NWI area exposed to the aqueous phase within the three-phase (air-water-NAPL) system. Using previously published relationships between interfacial areas and soil moisture contents, retardation factors for both AWI and NWI adsorption are shown to increase with decreasing soil moisture (or water saturation), in response to a corresponding increase in interfacial area within the range of moisture contents employed in the calculations. As an example, retardation factors for NWI adsorption of PFOA are shown to increase from a value of 1.86 at a water saturation of 77% to 44.6 at a water saturation of 17% (the assumed residual water saturation for this system). Within this range of moisture conditions, calculated AWI areas vary by a factor of 11.

Given the degree of variability in retardation factors anticipated for interfacial adsorption under unsaturated flow, we argue that the traditional use of retardation factors to estimate rates of contaminant transport is less reliable compared to their use in water-saturated flow conditions and that numerical methods are a better option for this purpose. A framework approach to implementing AWI adsorption into future or existing unsaturated flow and transport models is provided. For this purpose, it is important to note that the k_{ia} values presented herein are for individual PFCAs and that the $k_{ia}(C_w)$ relationship for a particular PFCA will likely vary when additional PFCAs are present in solution and at the AWI. The authors are currently conducting additional research to evaluate PFCA interfacial adsorption from solution mixtures. However, as observed by Vectis et al. (2008) for a mixture of PFOA and perfluorooctane sulfonate (PFOS), competitive adsorption processes favor the most surface-active solute, resulting in a surface tension isotherm for the mixture that closely follows that of the stronger surfactant as an individual solute. Therefore, the mathematical relationships proposed herein for implementing AWI adsorption within numerical simulators are anticipated to hold in the case of PFCA mixtures, as the continued applicability of the LS-equation to define the tension-concentration relationship can also be anticipated to hold.

Acknowledgements

This research was supported wholly (or in part) by the U.S. Department of Defense, through the Strategic Environmental Research and Development Program (SERDP). The authors wish to acknowledge Dr. Andrea Leeson (SERDP Environmental Restoration Program Manager) for her continued assistance with our research.

References

1. Adamson, A.W., Gast, A.P. *Physical Chemistry of Surfaces*, John Wiley & Sons, Inc., New York, 1997.
2. Anderson, R. H., Long, G. C., Porter, R. C., Anderson, J. K., 2016. Occurrence of select perfluoroalkyl substances at U.S. Air Force aqueous film-forming foam release sites other than fire-training areas: Field-validation of critical fate and transport properties. *Chemosphere*, 150, 678–685.
3. Anderson, R. H., Adamson, D.T., Stroo, H.F., 2019. Partitioning of poly- and perfluoroalkyl substances from soil to groundwater within aqueous film-forming foam source zones. *J. Contam. Hydrol.*, 220, 59-65.
4. ASTM Standard D1331, Standard Test Methods for Surface and Interfacial Tension of Solutions of Surface Active Agents. ASTM International, West Conshohocken, PA, 1989.
5. Batista, M.M., Guirardello, R., Krahenbuhl, M.A., 2015. Determination of Hansen solubility parameters of vegetable oils, biodiesel, diesel, and biodiesel-diesel blends. *J. Am. Oil Chem. Soc.*, 92, 95-109.
6. Bradford, S. A., Wang, Y., Torkzaban, S., and Simunek, J., 2015. Modeling the release of *E. coli* D21g with transients in water content, *Water Resour. Res.*, 51, 3303–3316, doi:10.1002/2014WR016566.
7. Brusseau, M.L., 1992. Rate-limited mass transfer and transport of organic solutes in porous media that contain immobile immiscible organic liquid. *Water Resour. Res.* 28, 33–45.
8. Brusseau, M. L., Popovicova, J., Silva, J. A. K., 1997. Characterizing gas-water interfacial and bulk water partitioning for transport of gas-phase contaminants in unsaturated porous media. *Environ. Sci. Technol.*, 31 (6), 1645–1649.
9. Brusseau, M.L., 2018. Assessing the potential contributions of additional retention processes to PFAS retardation in the subsurface. *Science of the Total Environment*, 613-614, 176-185.
10. Costanza, M.S., Brusseau, M.L., 2000. Influence of adsorption at the air-water interface on the transport of volatile contaminants in unsaturated porous media. *Environ. Sci. Technol.* 34, 1–11.
11. Costanza-Robinson, M.S. and Brusseau, M.L., 2002. Air-water interfacial areas in unsaturated soils: Evaluation of interfacial domains. *Water Res. Research*, 38(10), 13-1 – 13-7.
12. Costanza-Robinson, M.S., Harrold, K.H., Lieb-Lappen, R.M., 2008. X-ray microtomography determination of air-water interfacial area-water saturation relationships in sandy porous media. *Environ. Sci. Technol.*, 42(8), 2949-2956.
13. Downes, N., Ottewill, G.A., Ottewill, R.H., 1995. An investigation of the behavior of ammonium perfluoro-octanoate at the air/water interface in the absence and presence of salts. *Colloids Surf A Physicochem Eng Asp.*, 102, 203-211.
14. Filipovic, M., Woldegiorgis, A., Norström, K., Bibi, M., Lindberg, M., Österås, A.-H., 2015. Historical usage of aqueous film forming foam: A case study of the widespread

- distribution of perfluoroalkyl acids from a military airport to groundwater, lakes, soils and fish. *Chemosphere*, 129, 39–45.
15. Goss, K-U., 2008. The pKa values of PFOA and other highly fluorinated carboxylic acids. *Environ. Sci. Technol.*, 42(2), 456-458.
 16. Guelfo, J.L., Higgins, C.P., 2013. Subsurface transport potential of perfluoroalkyl acids at aqueous film-forming foam (AFFF)-impacted sites. *Environ. Sci. Technol.* 47, 4164-4171.
 17. Gurkov, T.D., Dimitrova, D.T., Marinova, K.G., Bilke-Crause, C., Gerber, C., Ivanov, I.B., 2005. Ionic surfactants on fluid interfaces: determination of the adsorption; role of the salt and the type of the hydrophobic phase, *Colloids Surf A Physicochem Eng Asp.*, 261, 29-38.
 18. Hansen, C. M., 2007. *Hansen Solubility Parameters: A Users Handbook*. 2nd Ed.. CRC Press, Boca Raton, FL.
 19. Higgins, C.P., Luthy, R.G., 2006. Sorption of perfluorinated surfactants on sediments. *Environ. Sci. Technol.* 40(23), 7251-7256.
 20. Houtz, E.F., Higgins, C.P., Field, J.A., Sedlak, D.L., 2013. Persistence of perfluoroalkyl acid precursors in AFFF-impacted groundwater and soil. *Environ. Sci. Technol.*, 47(15), 8187-8195.
 21. Kakare, M. V., Fort, T., 1996. Determination of the air-water interfacial area in wet “unsaturated” porous media. *Langmuir*, 12(8), 2041-2044, 1996.
 22. Kim, H., Rao, P.S.C, Annable, M.D., 1997. Determination of effective air-water interfacial area in partially saturated porous media using surfactant adsorption. *Water Res. Research*, 33(12), 2705-2711.
 23. Kim, H., Annable, M. D., Rao, P. S., 1998. Influence of air-water interfacial adsorption and gas-phase partitioning on the transport of organic chemicals in unsaturated porous media. *Environ. Sci. Technol.*, 32 (9), 1253-1259.
 24. Kim, H., Rao, P. S. C., Annable, M. D., 1999. Gaseous tracer technique for estimating air-water interfacial areas and interface mobility. *Soil Sci. Soc. Am. J.*, 63(6), 1554–1560.
 25. Kim, H., Annable, M. D., Rao, P. S. C., 2001. Gaseous transport of volatile organic chemicals in unsaturated porous media: effect of water-partitioning and air-water interfacial adsorption. *Environ. Sci. Technol.*, 35(22), 4457–4462.
 26. Kissa, E. 2001. *Fluorinated Surfactants and Repellents*, Surfactant Science Series, 97. Marcel Dekker, New York.
 27. Kovalchuk, N. M., Trybala, A., Starov, V., Matar, O., Ivanova, N., 2014. Fluoro- vs hydrocarbon surfactants: Why do they differ in wetting performance? *Adv. Colloid Interface Sci.*, 210, 65-71.
 28. Lunkenheimer, K., Prescher, D., Hirte, R., Geggel, K., 2015. Adsorption properties of surface chemically pure sodium perfluoro-n-alkanoates at the air/water interface: counterion effects within homologous series of 1:1 ionic surfactants. *Langmuir*, 31, 970–981.
 29. Lyu, Y., Brusseau, M.L., Chen, W., Yan, N., Fu, X., Lin, X., 2018. Adsorption of PFOA at the air-water interface during transport in unsaturated porous media. *Environ. Sci. Technol.*, 52(14), 7745-7753.

30. McKenzie, E.R., Siegrist, R.L., McCray, J.E., Higgins, C.P., 2016. The influence of a non-aqueous phase liquid (NAPL) and chemical oxidant application of perfluoroalkyl acid (PFAA) fate and transport. *Water Res.* 92, 199-207.
31. Moody, C.A., Field, J.A., 1999. Determination of perfluorocarboxylates in groundwater impacted by fire-fighting activity. *Environ. Sci. Technol.*, 33(16), 2800-2806.
32. Moody, C.A., Field, J.A., 2000. Perfluorinated surfactants and the environmental implications of their use in fire-fighting foams. *Environ. Sci. Technol.*, 34(18), 3864-3870.
33. Moody, C. A., Hebert, G. N., Strauss, S. H., Field, J. A., 2003. Occurrence and persistence of perfluorooctane sulfonate and other perfluorinated surfactants in groundwater at a fire-training area at Wurtsmith Air Force Base, Michigan, USA. *J. Environ. Monit.*, 5(2), 341–345.
34. Mukerjee, P., Handa, T., 1981. Adsorption of fluorocarbon and hydrocarbon surfactants to air-water, hexane-water, and perfluorohexane-water interfaces. Relative affinities and fluorocarbon-hydrocarbon nonideality effects. *J. Phys. Chem.*, 85(15), 2298-2303.
35. Peng, S., Brusseau, M.L., 2005. Impact of soil texture on air-water interfacial areas in unsaturated sandy porous media. *Water Resour. Res.* 41, W03021. <http://dx.doi.org/10.1029/2004WR003233>.
36. Porter, M.L., Wildenschild, D., Grant, G., Gerhard, J.I., 2010. Measurement and prediction of the relationship between capillary pressure, saturation, and interfacial area in a NAPL-water-glass bead system. *Water Resources Research*, 46, W08512, doi:10.1029/2009WR007786.
37. Psillakis, E., Cheng, J., Hoffmann, M.R., Colussi, A.J., 2009. Enrichment factors of perfluoroalkyl oxoanions at the air/water interface. *J. Phys. Chem. A Lett.* 113, 8826–8829.
38. Saripalli, P. K., Rao, P. S. C., Annable, M. D., 1998. Determination of specific NAPL-water interfacial areas of residual NAPLs in porous media using the interfacial tracers technique. *J. Contam. Hydrol.*, 30(3-4), 375-391.
39. Shin, H-M., Viery, V.M., Ryan, P.B., Detwiler, R., Sanders, B., Steenland, K., Bartell, S.M., 2011. Environmental fate and transport modeling for perfluorooctanoic acid emitted from the Washington Works Facility in West Virginia. *Environ. Sci. Technol.*, 45(4). 1435-1442.
40. Silva, J. A. K., 1997. Retention processes affecting VOC vapor transport in water-unsaturated porous media. Master's Thesis. University of Arizona, Tucson, AZ.
41. Silva, J. A. K., Bruant, R. G., Conklin, M. H., Corley, T. L., 2002. Equilibrium partitioning of chlorinated solvents in the vadose zone: Low foc geomeidia. *Environ. Sci. Technol.* 2002, 36(7), 1613-1619.
42. Szymczyk, K., Janczuk, B., 2007. The adsorption at solution-air interface and volumetric properties of mixtures of cationic and nonionic surfactants. *Colloids Surf A Physicochem. Eng. Asp.*, 293(1-3), 39-50.
43. U.S Environmental Protection Agency (EPA), 2002. Methods for measuring the acute toxicity of effluents and receiving waters to freshwater and marine organisms, 5th Ed., EPA-821-R-02-012. October.

44. Vectis, C.D., Park, H., Cheng, J., Mader, B.T., Hoffmann, M.R., 2008. Enhancement of perfluorooctanoate and perfluorooctanesulfonate activity at acoustic cavitation bubble interfaces. *J. Phys. Chem. C.*, 112(43). 16850-16857.
45. Vierke, L., Berger, U., Cousins, I.T., 2013. Estimation of the acid dissociation constant of perfluoroalkyl carboxylic acids through experimental investigation of their water-to-air transport. *Environ. Sci. Technol.*, 47(19), 11032–11039.
46. Weber, A.K., Barber, L.B., LeBlanc, D.R., Sunderland, E.M., Vectis, C.D., 2017. Geochemical and hydrologic factors controlling subsurface transport of poly- and perfluoroalkyl substances, Cape Cod, Massachusetts. *Environ. Sci. Technol.*, 51 (8), 4269–4279.
47. Xiao, F., Simcik, M.F., Halback, T.R., Gulliver, J.S., 2015. Perfluorooctane sulfonate (PFOS) and perfluorooctanoate (PFOA) in soils and groundwater of a U.S. metropolitan area: Migration and implications for human exposure. *Water Research*, 72, 64-74.